CNRS
Centre National de la Recherche Scientifique

INFN
Istituto Nazionale di Fisica Nucleare

Advanced Virgo single cavity alignment

VIR-109A-08

M. Mantovani

Issue: 1

Date: November 17, 2008

VIRGO * A joint CNRS-INFN Project
Via E. Amaldi, I-56021 S. Stefano a Macerata - Cascina (Pisa)
Secretariat: Telephone (39) 050 752 521 * FAX (39) 050 752 550 * Email W3@virgo.infn.it

Contents

1 Introduction **2**
1.1 Radiation pressure effect on the resonant frequency 2

2 Single cavity alignment error signals - increasing the power **3**
2.1 Low power regime 4
2.2 High power regime 5
2.2.1 Gouy phase optimization 5

3 Alignment Error signals **6**

4 Conclusions **6**

A Validation of Optickle - Single Cavity - low power regime **7**

1 Introduction

In this note the Alignment error signals for the single cavity system have been studied in presence of radiation pressure. The frequency domain simulation tool which will be used to study the alignment system of a single cavity is Optickle [1], in which the radiation pressure effect and the 01 modes propagation are included.

1.1 Radiation pressure effect on the resonant frequency

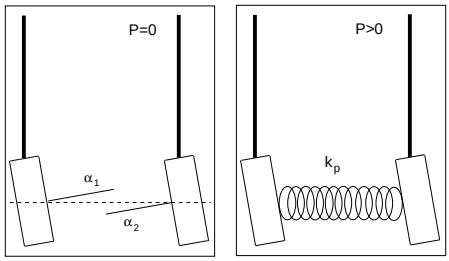

Figure 1: In this schematic the effect of the radiation pressure on a single cavity is shown. The effect of power stored in the cavity is equal to a spring which connects the two mirrors, thus the cavity mirrors are not decoupled anymore.

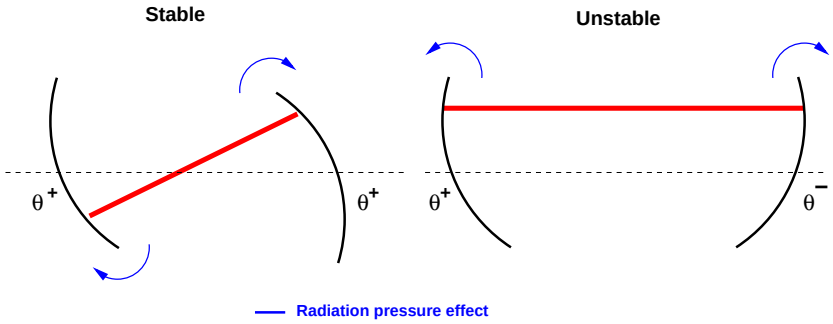

Figure 2: Angular modes present in a high power cavity. The radiation pressure cures the misalignment in the stable mode while pushes away the mirrors in the unstable mode.

In an high power Fabry-Perot cavity with suspended mirrors the effect of the radiation pressure varies the stiffness of the system [2] coupling the angular d.o.f. analogously to two single pendulum connected by a spring with an elastic constant k_{p}.
In the long cavity approximation the radiation pressure creates a component of additional stiffness k_{p} to the system which is, in a single cavity system, a 2×2 matrix:

$$k_p = \frac{2PL}{c\left(1 - g_1 \cdot g_2\right)} \begin{bmatrix} -g_2 & 1 \\ 1 & -g_1 \end{bmatrix} \tag{1}$$

which gives two frequency eigenvectors, which can be written as [3]:

$$\begin{aligned} f_{\mathrm{max}} &= \frac{1}{2\pi}\sqrt{\omega_0^2 + \frac{GP_{\mathrm{in}}L}{Ic}\frac{\left(-(g_1+g_2)+\sqrt{4+(g_1-g_2)^2}\right)}{(1-g_1g_2)}} \\ f_{\mathrm{min}} &= \frac{1}{2\pi}\sqrt{\omega_0^2 + \frac{GP_{\mathrm{in}}L}{Ic}\frac{\left(-(g_1+g_2)-\sqrt{4+(g_1-g_2)^2}\right)}{(1-g_1g_2)}} \end{aligned} \tag{2}$$

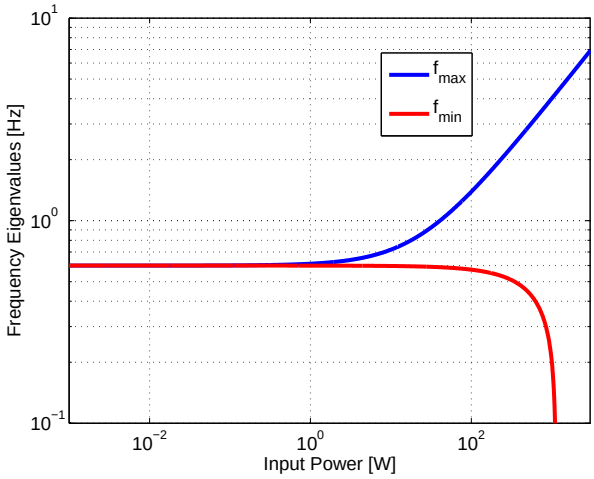

Figure 3: Shift of the resonance frequencies as a function of the input power. The system gets unstable for input powers bigger than ~ 1 kW.

In general the radiation pressure acts on the mirror angles restoring the alignment in the stable configuration, with a resonant frequency which grows with the power circulating in the cavity, as it is shown in Equation 2, while in the other mode the mirrors are pushed apart by the radiation pressure, lowering the frequency up to negative optical torque.
As it is shown in Figure 3 in the advanced Virgo single cavity optical set-up, only starting from very high input powers, ~ 1 kW, the mode defined *Unstable*, see Figure 2, has negative optical torque. In this case the negative frequency should be compensated by the control loop.
In the advanced Virgo single cavity case the system does not become unstable, since the input power is at maximum ~ 125 W, thus the mitigation of the negative optical torque is not needed, but it is still interesting to study the control quality in the high power regime, where the radiation pressure has a non negligible effect.

2 Single cavity alignment error signals - increasing the power

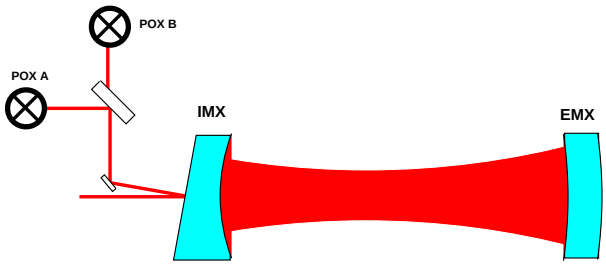

Figure 4: X-arm single cavity schematic. The Automatic Alignment error signals are detected at the cavity pick-off port, POX.

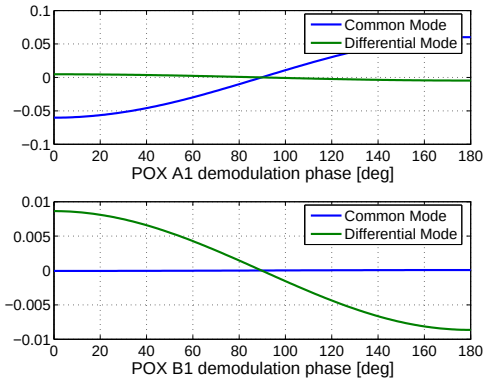

Figure 5: Common and Differential modes error signals detected with the two quadrant diodes at the POX detection port, with 90 deg of Gouy phase difference, for an input power of 10 mW.

Optical component	ROC [m]	T	L	Rar
IMX	1416	0.7 %	40 ppm	100 ppm
EMX	1646	5 ppm	40 ppm	0

Table 1: Table of the cavity optical parameters, [4] [5].

For the Advanced Virgo cavity alignment a Ward-like technique has been chosen. The error signal is constructed by using the IMX/Y pick-up beam (for each cavity), which can be extracted thanks to the input mirror wedge, demodulated at a modulation frequency which is resonating in the cavity ($f_{\mathrm{mod}} = 6270389.2$ [6]).

2.1 Low power regime

diode	demodulation frequency [MHz]	Gouy phase tuning [deg]
POX A	6.2703892	82
POX B	6.2703892	82 + 90

Table 2: Table of the cavity optical parameters.

In the low power regime the alignment system can be easily optimized by tuning the initial Gouy phase, by tuning a telescope in front of the diode set, in order to be able to detect with the two diodes (separated by 90 deg of Gouy phase shift) the two cavity modes.
The cavity modes can be defined as:

$$\begin{array}{lcl} \text{Differential} & = & \frac{(\theta_{\mathrm{EMX}}-\theta_{\mathrm{IMX}})}{2} \\ \text{Common} & = & \frac{(\theta_{\mathrm{EMX}}+\theta_{\mathrm{IMX}})}{2} \end{array} \tag{3}$$

In order to have the best decoupling between the two modes the Gouy phase has been optimized to obtain the best *controllability* for the control matrix [1].

[1] A quality criterion for a designed control system has been developed, which is based on the capability of the sensing scheme to sense the angular position of the d.o.f. to be controlled [8].

2.2 High power regime

If we consider the low power regime, we can have a nicely controllable system by optimizing the Gouy phases of the POX/Y detection ports, as it is shown in Figure 2.1.
An interesting point is to understand how much the optimization of an optical parameter, such as the Gouy phase, influences the control capability for different input powers.

2.2.1 Gouy phase optimization

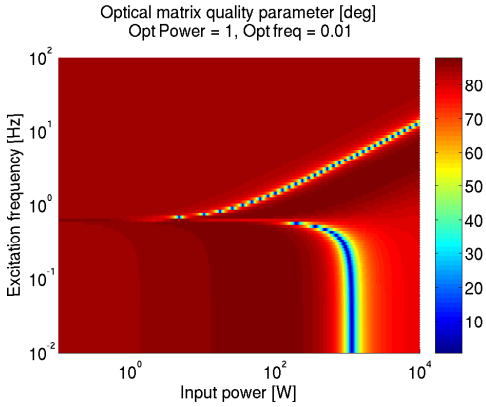

Figure 6: Control system quality parameter as a function of the input power and the excitation frequency; the Gouy phase has been optimized at the POX detection port for an input power of 1 W and an excitation frequency of 0.01 Hz. The 90 deg of quality parameter corresponds to a perfect decoupling, while 0 deg corresponds to an uncontrollable system.

The optimization of the Gouy phase is a hardware optimization, which requires the tuning of telescopes before the quadrant diode set, which can not be implemented during the lock acquisition, as opposed to the demodulation phase tuning which can be done remotely. Depending on the locking strategy a variable power lock acquisition can be implemented, thus it is important to understand how much the initial Gouy phase tuning influences the quality of the control system.
If we suppose to have a variable power lock acquisition, starting from a cold interferometer, it is useful to understand when the Gouy phase has to be optimized in order to have a good control system for all the possible input power configurations. As it is shown in the Figure 6, which represents the quality parameter of the alignment control system (0 means un-controllable system and 90 a perfectly controllable system), if the Gouy phase is tuned in the loop band in the cold interferometer state (10 mHz at 1 W) the system is well controllable for almost all the input power configurations.
The controllability get worse only in correspondence of the input power which brings the unstable mode to have negative optical torque, but the power is well above with respect the one proposed for advanced Virgo (∼1 kW with respect to 125 W).
In this simulation the tuning of the Gouy phase is done in order to maximize the decoupling of the cavity d.o.f., which requires also a demodulation phase tuning, only in regions where at least one of the two error signals has significant amplitude [2].
It is interesting to notice how much the decoupling between the d.o.f. to control can change as a function of the input power and excitation frequency, maintaining the same Gouy and demodulation phases settings.
From Figure 6 we can notice that the controllability remains almost optimal for all the input powers and excitation frequencies, except at the mechanical resonances. Thus we can conclude that the initial setting of

[2] the controllability of the system has been scanned in the Gouy and demodulation phase space neglecting the regions for which both signals have an amplitude smaller than a 30 % of the maximum amplitude, in order to exclude singular regions.

the Gouy phase of the pick-off diodes it is enough to allow a very good controllabilty of the cavity angular d.o.f. even if the input power is strongly increased.

3 Alignment Error signals

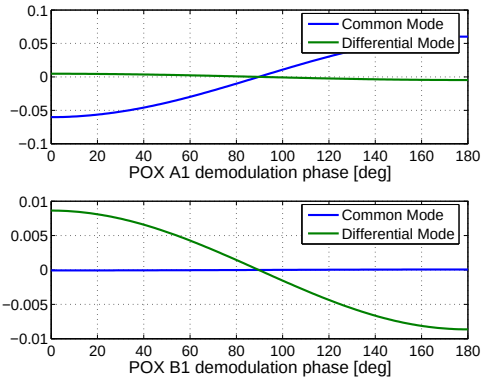

Figure 7: Common and Differential modes error signals detected with the two quadrant diodes, with 90 deg of Gouy phase difference, at the POX detection port for an input power of 10 mW. The optimized Gouy phase is 82 deg.

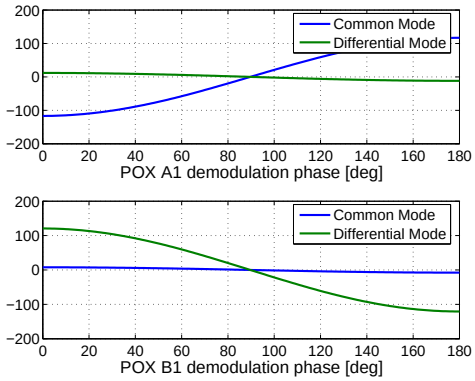

Figure 8: Common and Differential modes error signals detected with the two quadrant diodes, with 90 deg of Gouy phase difference, at the POX detection port for an input power of 125 W.

After the tuning of the Gouy phase, it is interesting to observe the error signal for low and high power (10 mW and 125 W). We can observe, from the plots in Figure 8, that the decoupling of the signal is slightly spoiled in the high power regime but it is still very good.

4 Conclusions

The Automatic Alignment control system for the Advanced Virgo cavities alignment can be done with a Ward-like technique. The diodes are placed at the pick-off port of the Input mirrors, which have wedges to allow the separation of the pick-off beam from the main beam, demodulated at the first modulation frequency for the advanced Virgo sensing scheme, $f_{\mathrm{mod1}} = 6270389.2$ [6]. This modulation frequency is resonating in the arm cavities.
The controllability of the system does not vary strongly as a function of the power and of the excitation frequency, tuning the optical parameters such as the demodulation and Gouy phases in the initial phase at medium power. We can conclude then that the alignment control for the single cavities in the high power interferometer can be easily implemented.

A Validation of Optickle - Single Cavity - low power regime

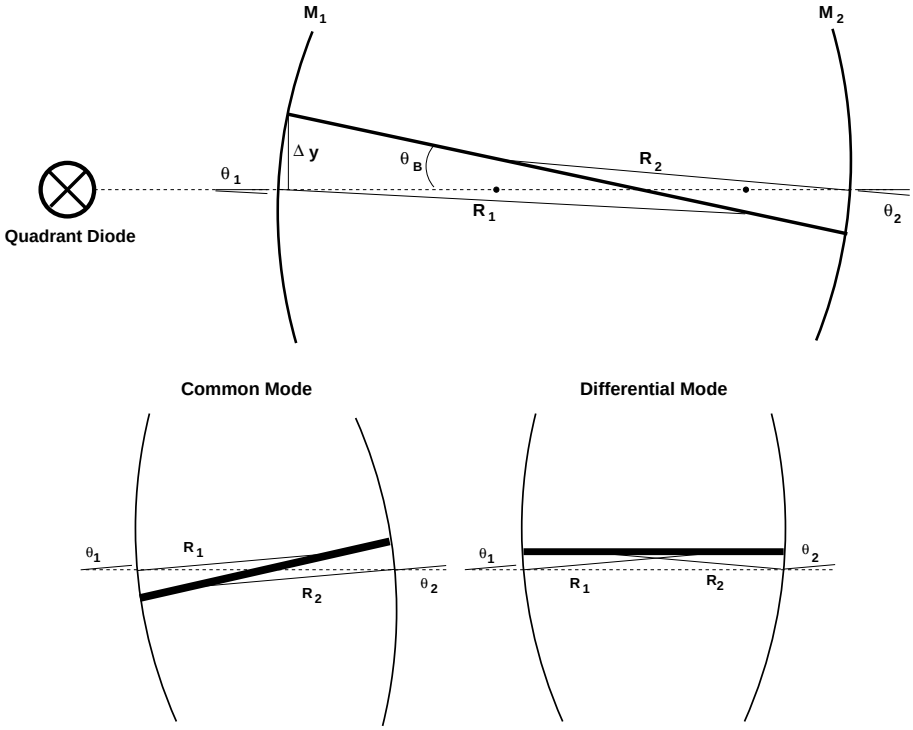

Figure 9: Schematic of a spherical single cavity of length L, in the bottom plot the effect of a differential and common displacement of the cavity mirrors on the beam are shown.

In order to validate the simulation tool Optickle, a generic single cavity has been modeled with Optickle and Finesse [7] and compared with the analytic results in the low power regime [3]. A spherical cavity of length L has been considered, as it is shown in Figure 9, where R_1 and R_2 are the radii of curvature of the input (M_1) and terminal mirror respectively (M_2).
The wave front sensor is placed in reflection to the cavity, we can compute the signal detected due to the translation and the tilt of the beam in the cavity with respect to the cavity axis at the input mirror.
If the two mirrors wold be misaligned by an amount θ_1 and θ_2 respectively [4], the beam will be tilted by an angle θ_B and translated by a quantity Δy.
The misalignment between the beam and the cavity axis can be written as:

$$\theta_{\mathrm{B}} = \arctan\left(-\frac{R_1 \sin\theta_1 + R_2 \sin\theta_2}{L - R_1\cos\theta_1 - R_2\cos\theta_2}\right) \tag{4}$$

and the translation is equal to:

$$\Delta y = R_1\left(\sin\theta_1 - \sin\theta_B\right) \tag{5}$$

$$\tag{6}$$

The error signal detected by a quadrant diode placed in reflection will be:

$$S = \sum_j A_j \Theta_j \cos(\Phi_{\mathrm{G}} - \Phi_{\mathrm{Gj}}) \cos(\phi_{\mathrm{dem}} + \phi_{\mathrm{demj}}) \tag{7}$$

[3] in order to compare the two simulation tools the radiation pressure effects have to be negligible, since these are not taken into account in the Finesse simulation, thus an input power of 4 mW has been chosen
[4] The angles are considered positive along the beam direction.

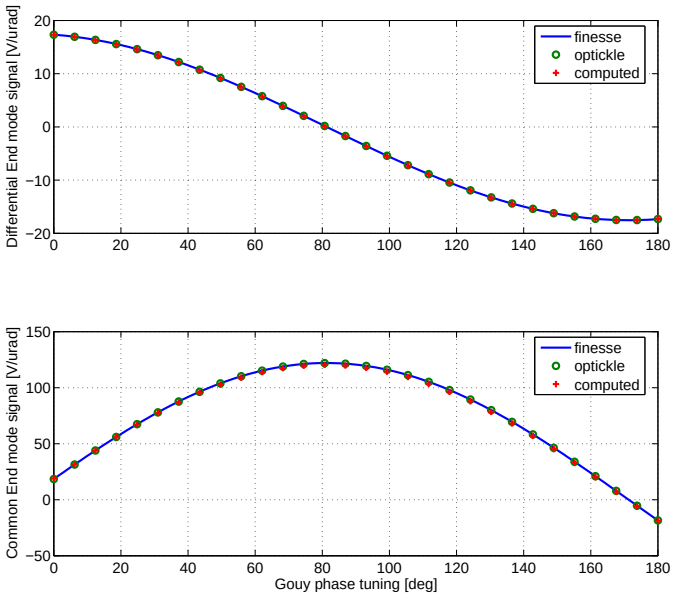

Figure 10: Comparison between the computed and simulated optical matrix elements (simulated with Finesse and Optickle) for the Differential and Common End mirror modes.

where A_j alignment sensing vector (which depends on the diode responsivity, gain, ...), Θ_j is the normalized mode angle [5], $\Phi_{\rm G}$ and Φ_{Gij} are the Gouy and intrinsic Gouy phases and $\phi_{\rm dem}$ and $\phi_{\rm demj}$ are the demodulation and intrinsic demodulation phases. We can explicitly re-write it.

$$S \propto A \left(\frac{\Delta y}{\omega_0} \cos(\Phi_{\rm G} - \Phi_{\rm G(shift)}) + \frac{\pi \theta_{\rm B} \omega_0}{\lambda} \cos(\Phi_{\rm G} - \Phi_{\rm G(tilt)}) \right) \cos(\phi_{\rm dem}) \tag{8}$$

Thus the wave front sensor signal analytical results have been compared with the simulation results obtained with Finesse and Optickle for the two cavity modes, differential and common modes, as a function of the diode Gouy phase.

From the Figure 10 the two simulation tools show a good agreement, even if there is a small amplitude discrepancy between the Finesse and Optickle results (of about 7 %). In this note the Optickle simulation tool has been used since the aim of this note is to study the radiation pressure effect on the two cavity mode alignment error signals.

References

[1] Optickle home-page $http://ilog.ligo-wa.caltech.edu:7285/advligo/ISC_Modeling_Software$ 2

[2] D. Sigg *et al.*, *Phys. Lett. A* **354** 3 (2006) 167-172 . 2

[3] Mode calculation based on Sigg's radiation pressure induced instability model Ligo note T070276-00-Z 2

[4] M. Mantovani, A. Freise, "Initial set of optical parameters for numerical simulations towards Advanced Virgo" Virgo note VIR-002B-07 4

[5] the normalized angle mode corresponds to $\Theta = \frac{\Delta y}{\omega_0}$ for translation of the beam an $\Theta = \frac{\pi \theta_{\rm B} \omega_0}{\lambda}$ for the tilt of the beam, where ω_0 is the beam waist and λ is the wavelength.

[5] Virgo Collaboration, "Advanced Virgo Preliminary Design" VIR-089A-08 4

[6] G. Vajente, "Simulation of Advanced Virgo Length Sensing and Control system" Virgo note VIR-068A-08 4, 6

[7] A. Freise, G. Heinzel, H. Luck, R. Schilling, B. Willke and K. Danzmann, "Frequency domain interferometer simulation with higher-order spatial modes", Class. Quant. Grav. **21** (2004) S1067 [arXiv:gr-qc/0309012]. 7

[8] M. Mantovani, A. Freise, "Evaluation of Alignment Sensing Matrices using Row Vector Orientation", proceedings of the 7^{th} Amaldi Conference, Sidney 2007. 4